

Research Article

Study on the Influence of AC Stray Current on X80 Steel under Stripped Coating by Electrochemical Method

Yanyu Cui , Tao Shen, and Qingmiao Ding 

Airport School, Civil Aviation University of China, Tianjin, China

Correspondence should be addressed to Yanyu Cui; yycui@cauc.edu.cn

Received 27 January 2019; Revised 18 March 2019; Accepted 26 March 2019; Published 9 April 2019

Academic Editor: Ramazan Solmaz

Copyright © 2019 Yanyu Cui et al. This is an open access article distributed under the Creative Commons Attribution License, which permits unrestricted use, distribution, and reproduction in any medium, provided the original work is properly cited.

The effect of AC stray current density on corrosion behavior of X80 steel with stripped coating defects was studied by electrochemical method. The experimental results showed that the open circuit potential of X80 steel was shifted negatively due to the existence of AC interference. The degree of negative shift increased with the increasing of AC stray current density. And the potential after the cut of AC interference was still more negative than before. That is, the corrosion interference continued after cutting the AC power. In the initial stage of the experiment, the corrosion current density with 30A/m^2 AC stray current interference was about 1.4 times of that without AC interference, while the corrosion current density with 50A/m^2 AC stray current interference was about two times of that without AC interference.

1. Introduction

With the rapid development of economy, the country's demand for energy is growing. Due to the high population density and the lack of land resources in China, it is inevitable that high-voltage transmission lines or railway systems and oil and gas pipelines crossover or long-distance parallel "public corridors" will be erected [1, 2]. Alternating current power generated by high-voltage transmission lines and railway systems is prone to AC corrosion of pipeline steel [3–6]. The presence of AC may break through the insulation of the pipeline to accelerate the corrosion and destruction of the pipeline, and threaten personal safety [7–10].

As the problem of AC corrosion of buried pipelines becomes more and more prominent, domestic and foreign scholars have conducted a lot of research about the effect of AC stray current on pipeline corrosion. The study found that the AC corrosion rate is not directly affected by the AC voltage, and the main role is the AC frequency and AC current density [11]. Liu Cheng et al. [12] studied the influence of AC stray current on the corrosion of X80 steel under different current densities by weight loss method, SEM, XRD, and EDS. It is found that with the AC stray current density increasing the corrosion rate of X80 steel increases slowly, then rapidly, and finally the increasing trend slows down.

Meanwhile, the forms of corrosion change from uniform corrosion to localized corrosion. Fu An qing [13] studied the influence of AC stray current on the corrosion behavior of X65 steel by electrochemical method and weight loss method. Coated pipeline steels with small size coating defects have a high risk of AC stray current corrosion. Under the interference of fixed AC current, the amplitude of the current on the polarization curve is inversely proportional to the square of the defect diameter. Funk et al. [14] conducted field tests of $10\sim 30\text{A/m}^2$ and $300\sim 1000\text{A/m}^2$ on samples with an exposed area of 10cm^2 in sand and clay. The results show that if the current density at constant cathodic protection is 2A/m^2 , when the AC density is more than 30A/m^2 , the corrosion rate will over 0.1mm/a . Goidanich et al. [15] obtained an experimental result that the AC corrosion rate is twice the self-corrosion rate of the undisturbed current sample at a current density of 10A/m^2 ; when the AC current density exceeds 30A/m^2 , the corrosion rate increases exponentially. Wen C et al. [16] found that the quantity, area, and depth of the corrosion pits arise with the increase of the AC current density. Zhu M et al. [17] found that, with the increasing AC current density, the corrosion degree of steel increases and the pits become more apparently. Dai NAW et al. [18] found that the high-amplitude alternating voltage interferences with 50

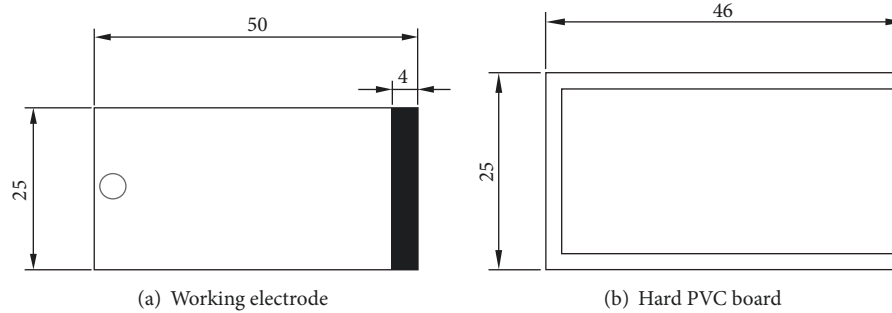


FIGURE 1: The diagram of the device.

TABLE 1: The composition of soil simulated solution.

Component	Content
distilled water/mL	1000
Na ₂ CO ₃ /g	0.1600
NaCl/g	0.5125
Na ₂ SO ₄ /g	0.1712
Na ₂ HCO ₃ /g	0.0865

and 100 Hz induce big pits on DSS 2205 samples; the pitting corrosion however is inhibited with further increasing the frequency. In general, the corrosion rate of metal increases with the increase of AC current density and decreases with time, but the magnitude of increase in different corrosion systems is different [19].

Most of the above studies are about the influence of AC stray current on the corrosion behavior of bare metal pipeline steel, without considering the influence of coating, and the experimental device adopts the traditional rectangular gap configuration and wedge-shaped gap configuration experimental device, which is different from the actual engineering. In the research of this paper, the experimental equipment has been improved. The electrochemical method is used to study the influence of AC stray current on the corrosion behavior of buried metal pipelines with peeling coating defects, which provided a certain reference for the safe operation of pipeline steel.

2. Experimental Method

2.1. Solution Preparation. The soil simulated solution is taken from the soil around an oil pipeline in Tianjin and centrifuged. After measurement by titration, the chemical composition was finally obtained as shown in Table 1.

2.2. Electrode Preparation. X80 pipeline steel hanging piece is selected as the experimental material, with a size of 50mm×25mm×2mm, and the chemical composition of X80 pipeline steel is shown in Table 2.

The simulated coating stripping device is composed of plexiglass boards, 0.5mm thick hard PVC boards, and hanging pieces, as shown in Figure 1. The rigid PVC board is used to simulate the peeling gap thickness, and the area of the hanging piece of 48 mm×21 mm is reserved as the

working area, and the remaining five sides were sealed with epoxy resin.

2.3. Experimental Content. The effects of AC stray current density on the corrosion behavior of X80 pipeline steel with peeling coating defects were investigated by testing the electrochemical parameters such as open circuit potential, polarization curve, and electrochemical impedance of the working electrode.

The working electrode is immersed in the prepared soil simulated solution, and sinusoidal wave signal is applied to the working electrode. The frequency is set at 50 Hz. The AC current density is 0 A/m², 30 A/m², and 50 A/m². One end of signal is connected with the carbon rod and the other end is connected with the working electrode. The test time is 11 days.

The electrochemical test uses standard-three-electrode system. In this system, specimens of X80 pipeline steel are tested as working electrode (WE), a platinum plate is used as the counter electrode (CE-Pt), and a saturated calomel electrode (SCE) is the reference electrode (RE). And graphite electrode is used to exert AC interference. In the electrochemical test, a series capacitor is added to the alternating current signal to prevent the electrochemical test system from interfering with the alternating current signal. The reference electrode of electrode potentials throughout the paper is SCE. The electrochemical test device is shown in Figure 2.

There are three processes for testing open circuit potentials: (1) potential test before AC density is applied; (2) potential test when alternating current density is applied; (3) potential test after AC density is removed.

The electrochemical impedance spectroscopy test frequency was 0.1 Hz-100 kHz with an amplitude of 10 mV, and the impedance spectrum was fitted by software of ZSimp Win.

The scan range of the polarization curve is ±400 mV (relative to the open circuit potential) and the scan rate is 1 mV/s.

3. Results and Discussion

3.1. Analysis of Eocp-Time. The variation of the working electrode potential over time at different AC current densities is shown in Figure 3. Each curve is divided into three stages, of which 0~600s is the potential without AC

TABLE 2: The chemical composition of X80 pipeline steel (quality)%.

C	Si	Mn	Cr	Mo	Ni	Al	Cu	Nb	Ti	Pb	Fe
0.042	0.189	1.560	0.028	0.243	0.230	0.034	0.153	0.060	0.019	0.005	rest

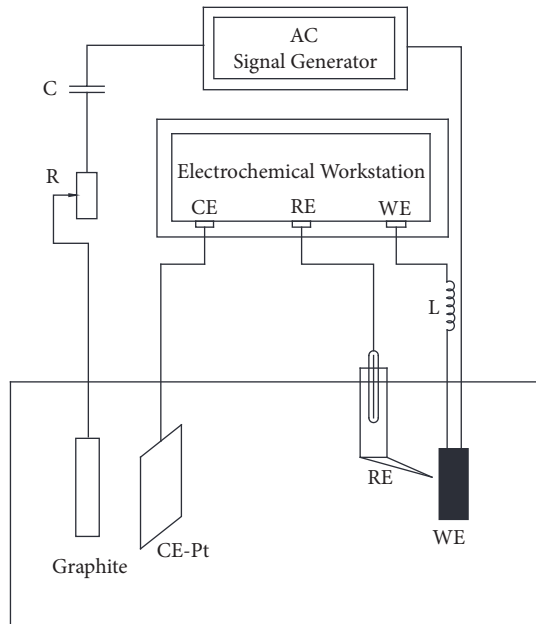


FIGURE 2: The diagram of the electrochemical test device.

interference, 600~1200s is the potential under the alternating current interference, and 1200~1800s is the potential after the alternating current is removed. As can be seen from Figure 3, when alternating current is not applied, the potential of the working electrode is about -0.66 V when it is just immersed in the solution and it is stabilized at -0.68 V with the prolongation of test time. At the moment when the alternating current is applied, it can be seen that the potential of the working electrode has a certain negative shift. When the applied alternating current density is 30 A/m², the instantaneous potential for applying alternating current is suddenly decreased from -0.65 V to -0.72 V, and the instantaneous potential for removing the alternating current is shifted to -0.69 V. When the applied alternating current density is 50 A/m², the instantaneous potential for applying alternating current suddenly drops from -0.67V to -0.79V and finally is stabilized at about -0.80V. When the AC power is removed, the potential is moving to -0.71V. It can be found that the negative potential deviation of 50A/m² is greater than 30A/m². And the potential of 30 A/m² is closer to the potential without alternating current than that of 50 A/m², but it is still lower than the potential without alternating current. It shows that the application of AC interference affects the working electrode potential obviously. The interference of potential is more obvious with the increasing of AC current density. It is that the supplement of electricity consumed by the system electrode reaction which indirectly accelerates the progress of the reaction. The

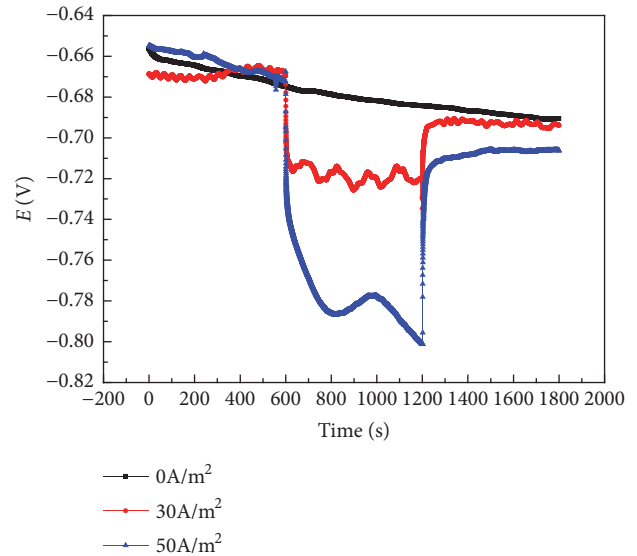


FIGURE 3: The diagram of Eocp-t under different AC current densities.

additional power increases with the increasing of the applied AC current density, and the effect on the reaction will be greater. Secondly, due to the influence of the electric field generated by the AC interference, the positive and negative charge layers accumulate more electrons than without the AC interference, which increases the interface electric field between the electrode/solution phases and accelerates the anodic dissolution and exfoliation the product film of the X80 electrode.

3.2. Analysis of Polarization Curve. The polarization of X80 steel without AC and in 30 A/m² and 50 A/m² is shown in Figure 4. The open circuit potential is a measure of the thermodynamic trend of metal corrosion reaction. The greater the potential difference between the cathode and the anode when the potential is negative, the greater the metal is to be corroded. It can be seen from Figure 4 that the open circuit potentials have a certain degree of negative shift with the progress of the experiment in three cases, which indicates that the tendency of the X80 steel to be corroded significantly increases with the progress of the experiment. At the beginning of the experiment, the fluctuation of the open circuit potential is obvious. With the progress of the experiment, the fluctuation of the open circuit potential becomes gentle and the heterogeneity reduces.

The corrosion current density of X80 steel without AC and with the AC interference of 30 A/m² and 50 A/m² is shown in Figure 5. The electrochemical parameters fitted from polarization curves under different AC current densities are shown in Table 3. And the corrosion current density is

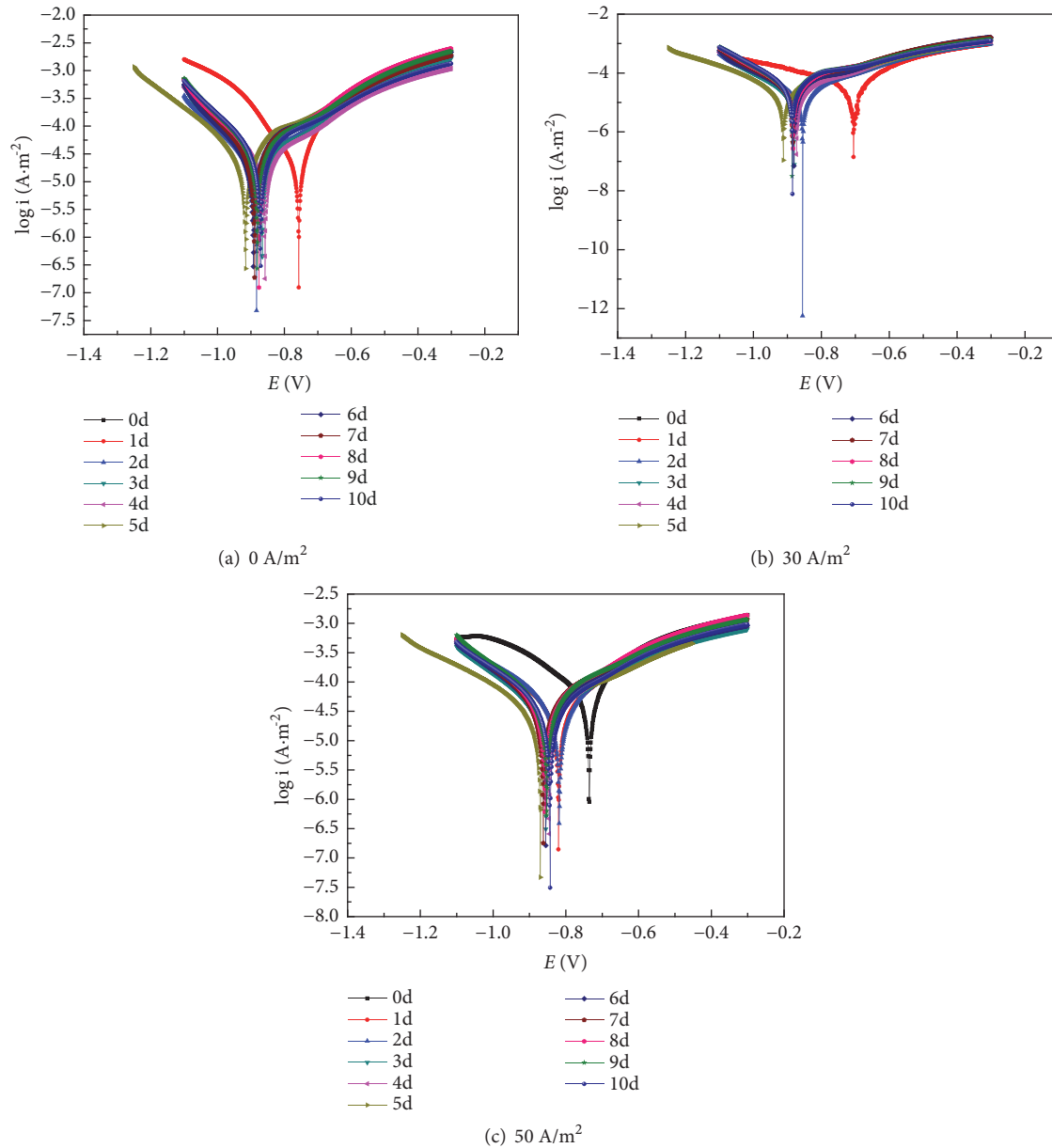


FIGURE 4: Polarization curve under different AC current densities.

obtained by dividing the corrosion current by the working area.

According to Figure 5 and Table 2, the corrosion current density at the beginning of the experiment is $49 \mu\text{A/cm}^2$ without AC stray current. At the moment of applying alternating current, the corrosion current density is up to $93 \mu\text{A/cm}^2$ with the AC interference of 50 A/m^2 and the corrosion current density is about twice than that without AC. While the corrosion current density is up to $66 \mu\text{A/cm}^2$ with the AC interference of 30 A/m^2 , the corrosion current density is about 1.4 times than that without AC. That is, at the moment of applying AC stray current, the oscillation of the alternating current increases the electrochemical activity of the working electrode and accelerates the corrosion rate of the metal. At

the beginning of the experiment, the surface oxygen content of the electrode is relatively high and the surface of the working electrode is clean and free of corrosion products. At this time, the contact between the electrode and the surrounding simulated solution is good, which is favorable for ion exchange.

From the second day to the eighth day of the experiment, the corrosion current density decreased to a certain extent compared with the beginning of the experiment, and there is a small fluctuation. This is because as the experiment progresses, oxygen is consumed. Oxygen diffusion is slower, corrosion products start to form on the electrode surface and have a certain degree of accumulation, and the accumulation of corrosion products at the damage point of the

TABLE 3: Electrochemical parameters fitted from polarization curves under different AC current densities.

AC interference (A/m ²)	Time (d)	Open circuit potential (V)	Corrosion current density ($\mu\text{A}/\text{cm}^2$)
0	0	-0.624	48.99
	2	-0.810	26.62
	9	-0.881	40.32
30	0	-0.663	65.69
	2	-0.855	21.31
	9	-0.891	44.84
50	0	-0.730	93.11
	2	-0.842	46.25
	9	-0.882	40.20

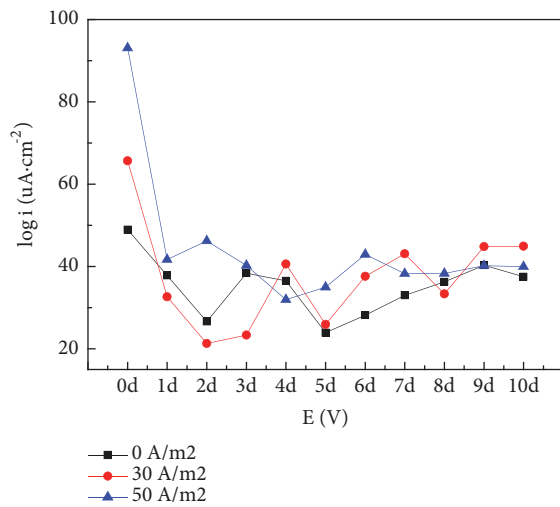


FIGURE 5: Relationship of corrosion current density with time under different AC current densities.

coating is particularly obvious. At this stage, oxygen diffusion and accumulation of corrosion products lead to a rapid decline of corrosion current density. The corrosion current density remained essentially unchanged as the experiment progressed to the ninth day. The application of an alternating current of $30\text{A}/\text{m}^2$ is greater than the application of an alternating current density of $50\text{A}/\text{m}^2$. This is probably because the application of the alternating current density of $50\text{A}/\text{m}^2$ in the previous corrosion process produces more corrosion products and accumulates in the defect of the peeling coating, making it difficult for the AC stray current to enter and the corrosion current density is lower than when the AC current density of $30\text{A}/\text{m}^2$ is applied. Overall, the corrosion current density increases with the increase of the applied AC current density, but the corrosion current density does not differ much in the later stage of corrosion.

3.3. Analysis of EIS. Figure 6 is the AC impedance spectra of X80 steel without AC and with AC current density of $30\text{A}/\text{m}^2$ and $50\text{A}/\text{m}^2$. It can be seen from Figure 6 that the high-frequency capacitive reactance arc in the impedance

spectrum does not start from the zero point and does not coincide. This is because the damaged area at the breakage point of the coating is large and the solution supply is sufficient after the coating is peeled off. The peeling gap is narrow and the ion concentration is low, so that the solution resistance in the slit is very large and the high-frequency capacitive reactance arc in the measured electrochemical impedance spectrum does not start from zero and does not coincide [20, 21]. The high-frequency impedance spectrum partially reflects the corrosion product information on the electrode surface, while the low-frequency impedance spectrum partially reflects the electrode reaction information. It can be seen from Figure 6(a) that the high-frequency capacitive antiarc radius of the ninth day of the experiment is not greater than the capacitive antiarc radius of the other experimental stages when stray current is not applied, which may be because as the soaking time is extended, the corrosion product film is formed on the surface of the sample to increase the impedance modulus, making the reaction difficult to perform, and the corrosion resistance is enhanced. After soaking for 1d, the inductive reactance is mainly caused by the adsorption of corrosion products. It can be seen from Figure 6(b) that as the AC stray current density of $30\text{A}/\text{m}^2$ is applied, the capacitive antiarc radius has a decreasing trend as a whole. It shows that, during the experiment, the oscillation of the alternating current prevents the corrosion product film from adhering well to the surface of the X80 steel substrate, so that the surface corrosion product film is later separated from the X80 steel matrix. It can be seen from Figure 6(c) that as an AC stray current density of $50\text{A}/\text{m}^2$ is applied, the radius of the capacitive arc increases and then decreases with the immersion time. This may be due to the accumulation of the precursor film leaving the X80 steel matrix at a later stage under the action of alternating current oscillations.

An electrode circuit is represented by an equivalent circuit composed of electrical components to accurately analyze the electrochemical impedance spectrum, as shown in Figure 7. Among them, R_s represents solution resistance, C_f is the capacitance of adsorption film formed on corroded metal surface, R_f is the resistance of adsorption film formed on corroded metal surface, C_d is the capacitance of double layer between metal surface and electrolyte solution, and R_p

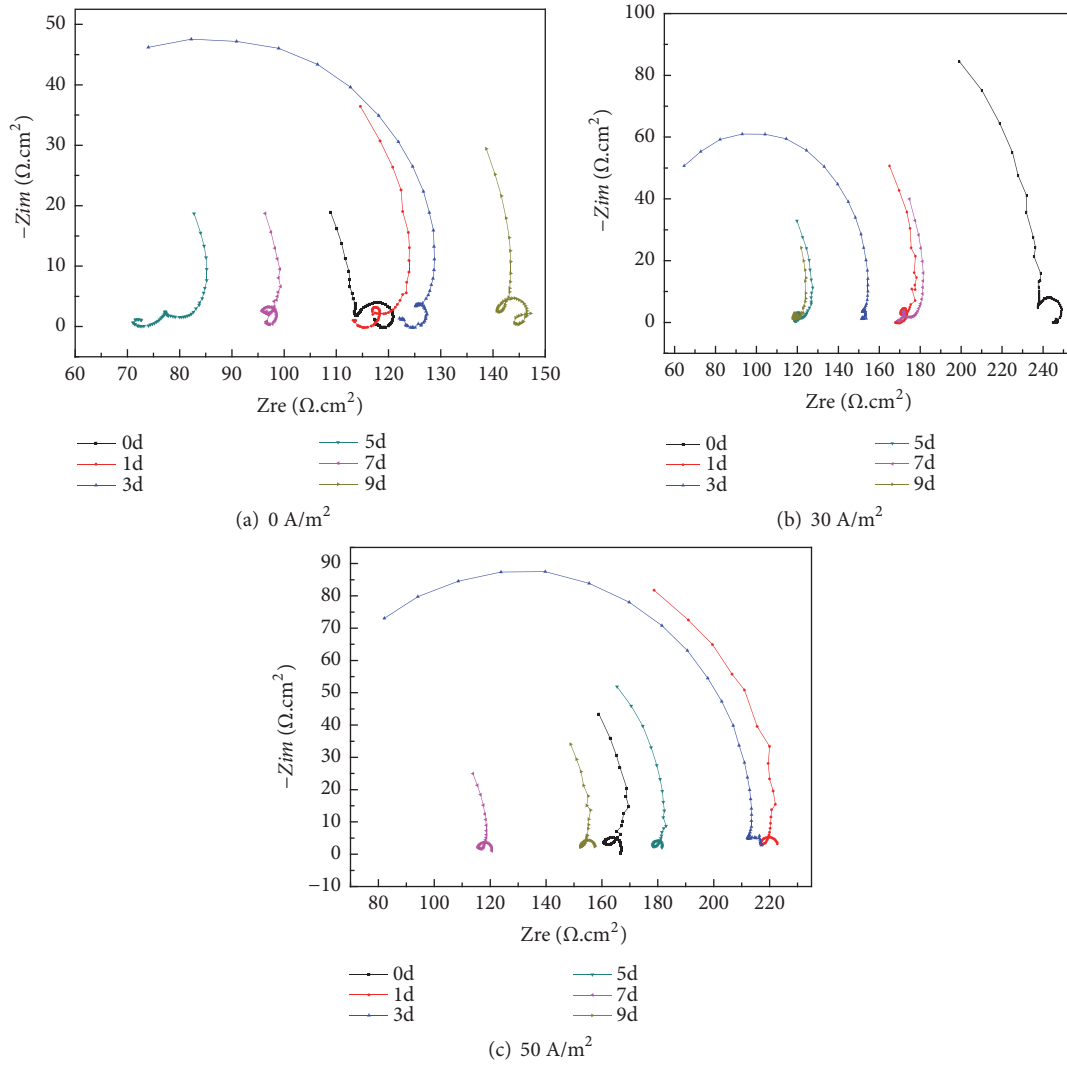


FIGURE 6: Electrochemical impedance spectroscopy under different AC current densities.

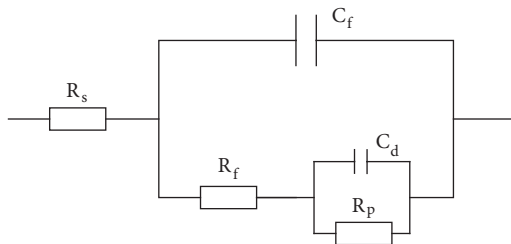


FIGURE 7: Equivalent circuit.

is the polarization resistance. It is related to Faraday process and anodic reaction, so it can well reflect corrosion and R_p is used to characterize corrosion rate [22]. Take the first, the second, and the ninth day as examples for analysis. The Bode diagrams and the fitting results of polarization resistance are shown in Figure 8 and Table 4.

The Bode amplitude-frequency characteristic curves in Figure 8 reflect the corrosion resistance of the metal. It

TABLE 4: Polarization resistance values under different AC interference.

Time (d)	AC interference (A/m^2)	R_p (Ω)
0		5.614
2	0	8.685
9		4.132
0		9.063
2	30	8.613
9		5.038
0		12.21
2	50	11.27
9		3.386

can be seen from the Bode diagrams that the amplitude-frequency curve has large fluctuations when there is no AC interference. After applying AC interference, the amplitude-frequency curves are smoother and the variation range is

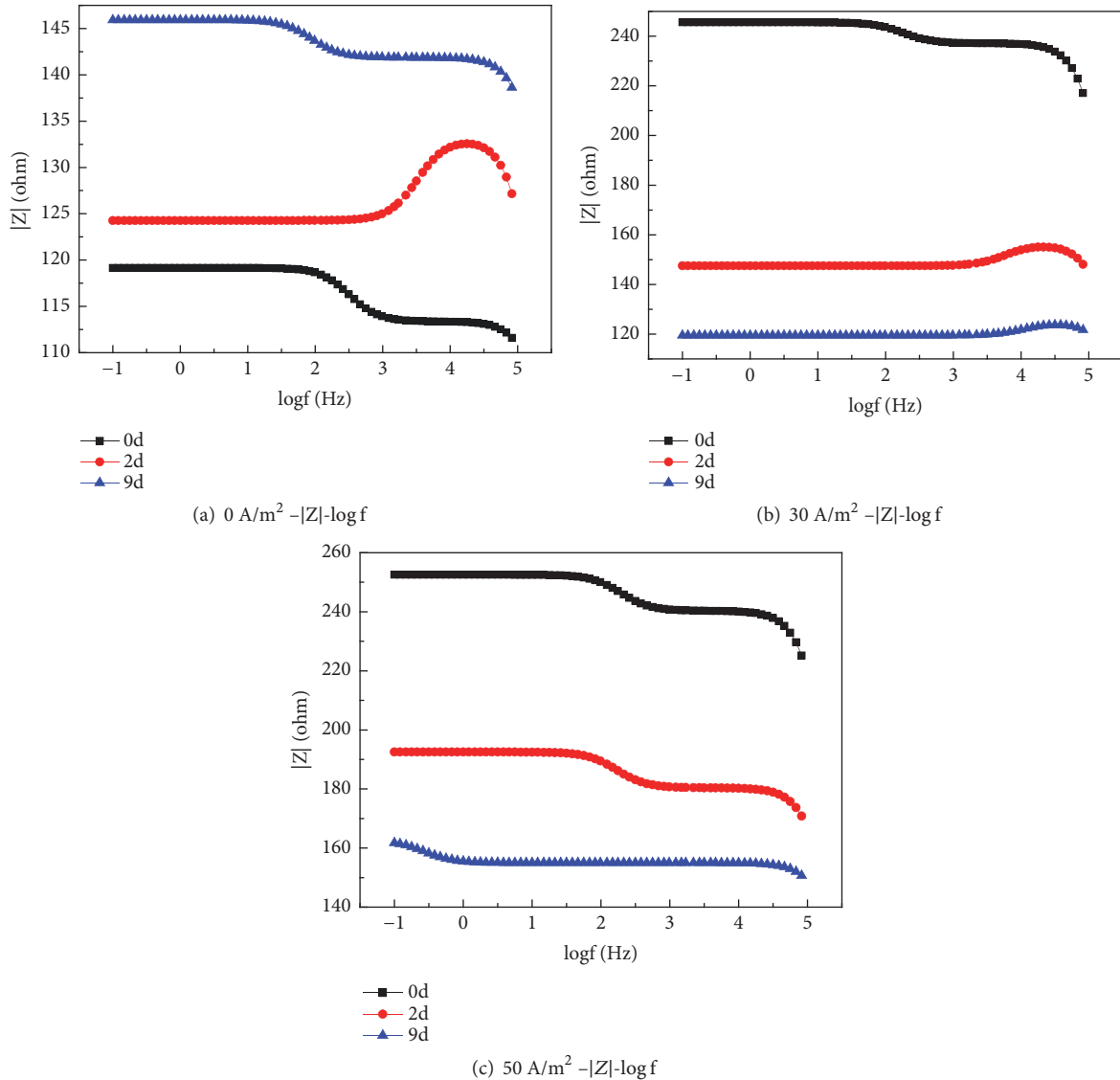


FIGURE 8: Bode plots under different AC current densities.

smaller. It shows that the corrosion resistance of the metal deteriorates after the application of the AC interference.

Table 4 shows the fitting results of polarization resistance without AC and with AC current density of 30 A/m^2 and 50 A/m^2 . Table 3 shows that if without applying AC stray current the polarization resistance increases and then decreases without applying AC stray current. That is to say, the resistance of metal corrosion increases first and then decreases, and the corrosion rate decreases first and then increases. When the AC current density is 30 A/m^2 and 50 A/m^2 , the polarization resistance decreases, which indicates that the corrosion degree of the metal under the stripping coating increases gradually with the experiment.

4. Conclusion

(1) The existence of AC interference makes the potential of X80 steel shift negatively to a certain extent, and the greater applied AC current density the more negative shift, indicating

that AC can accelerate corrosion of X80 steel. After disconnecting AC interference, the potential is still more negative than before, which indicates that the corrosion interference is continuing after disconnecting AC, and further illustrates the irreversibility of AC corrosion.

(2) With or without AC interference, the open circuit potential fluctuated obviously at the beginning of the experiment. With the experiment proceeding, the nonuniformity of open circuit potential decreased and the fluctuation is no longer intense.

(3) Under the influence of alternating current, the corrosion current density at AC interference of 30 A/m^2 and 50 A/m^2 is about 1.4 times and 2 times that of without AC interference. But in the later stage of corrosion, the corrosion current density is a little different. And the result of impedance is consistent with that of polarization. The corrosion resistance of the metal deteriorates after the application of the AC interference.

Data Availability

The research data used to support the findings of this study are included within the article.

Conflicts of Interest

The authors declare that there are no conflicts of interest regarding the publication of this article.

Acknowledgments

The research work was supported by Civil Aviation Safety Capacity Building Fund (construction of safety evaluation system for multibranch complex annular apron pipe network) and Airport Engineering Research Base Open Fund (study on the optimization of cathodic protection model in the apron area based on BEASY).

References

- [1] G. Yang, "Mitigation of AC interference on oil and gas pipelines due to single-phase earth fault in AC transmission line," *Corrosion Protection*, vol. 37, no. 2, pp. 165–170, 2016.
- [2] X. H. Yang, J. H. Chen, S. X. Hu et al., "Field test of electromagnetic effect on petroleum & gas pipeline due to AC transmission line," *Corrosion Protection*, vol. 33, S2, pp. 23–29, 2012.
- [3] H. Qin M, Y. Du X, and X. Lu M, "Research progress in corrosion of buried pipeline under dynamic DC stray current interference from urban rail transit," *Corrosion Science and Protection Technology*, vol. 30, no. 06, pp. 653–660, 2018.
- [4] B. Tribollet and M. Meyer, "2- AC- induced corrosion of underground pipelines," in *Undergr Pipeline Corrosion*, M. Orazem, Ed., vol. 35, Woodhead Publishing Limited, Amsterdam, Netherlands, 2014.
- [5] F. Roger, "Testing and mitigation of AC corrosion on 8 line: a field study," in *Corrosion*, NACE International, New Orleans, La, USA, 2004.
- [6] R. Zhang, P. R. Vairavanathan, and S. B. Lalvani, "Perturbation method analysis of AC-induced corrosion," *Corrosion Science*, vol. 50, no. 6, pp. 1664–1671, 2008.
- [7] R. G. Wakelin and C. Sheldon, "Investigation and mitigation of AC corrosion on a 300 MM natural gas pipeline," in *Corrosion*, vol. 972, NACE International, New Orleans, La, USA, 2004.
- [8] M. Zhu, C. Du, X. Li et al., "Effect of AC current density on stress corrosion cracking behavior of X80 pipeline steel in high pH carbonate/bicarbonate solution," *Electrochimica Acta*, vol. 117, pp. 351–359, 2014.
- [9] D. Tang, Y. Du, X. Li, Y. Liang, and M. Lu, "Effect of alternating current on the performance of magnesium sacrificial anode," *Materials and Corrosion*, vol. 93, pp. 133–145, 2016.
- [10] M. Zhu, C. Du, X. Li, Z. Liu, H. Li, and D. Zhang, "Effect of AC on stress corrosion cracking behavior and mechanism of X80 pipeline steel in carbonate/bicarbonate solution," *Corrosion Science*, vol. 87, pp. 224–232, 2014.
- [11] S. Goidanich, L. Lazzari, and M. Ormellese, "AC corrosion - Part 1: Effects on overpotentials of anodic and cathodic processes," *Corrosion Science*, vol. 52, no. 2, pp. 491–497, 2010.
- [12] C. Liu, Y. B. Guo, D. G. Wang et al., "Effects of alternating stray current on corrosion behavior of X80 pipeline steel," *Corrosion Protection*, vol. 36, no. 3, pp. 213–217+229, 2015.
- [13] F. U. Anqing, L. Naixin, B. Zhenquan et al., "Impacts of AC stray current on the corrosion behavior of pipe steel for long-distance pipeline," *Oil & Gas Storage & Transportation*, vol. 33, no. 7, pp. 748–756, 2014.
- [14] D. Funk, W. Prinz, and H. Schoneich, "Investigations of AC corrosion in cathodically protected pipes," *Ochrona Przed Korozja*, vol. 36, no. 10, pp. 225–228, 1993.
- [15] S. Goidanich, L. Lazzari, and M. Ormellese, "AC corrosion. Part 2: Parameters influencing corrosion rate," *Corrosion Science*, vol. 52, no. 3, pp. 916–922, 2010.
- [16] C. Wen, J. Li, S. Wang, and Y. Yang, "Experimental study on stray current corrosion of coated pipeline steel," *Journal of Natural Gas Science and Engineering*, vol. 27, pp. 1555–1561, 2015.
- [17] Z. Min, Y. Yongfeng, Z. Qiang et al., "Influence of AC interference on crack initiation behavior of pipeline steel in high pH solution," *International Journal of Electrochemical Science*, vol. 14, no. 1, pp. 1876–1883, 2019.
- [18] N. Dai, J. Wu, L. Zhang et al., "Alternating voltage induced oscillation on electrochemical behavior and pitting corrosion in duplex stainless steel 2205," *Materials and Corrosion*, vol. 70, no. 3, pp. 419–433, 2019.
- [19] L. W. Wang, X. H. Wang, Z. Y. Cui, Z. Y. Liu, C. W. Du, and X. G. Li, "Effect of alternating voltage on corrosion of X80 and X100 steels in a chloride containing solution - Investigated by AC voltammetry technique," *Corrosion Science*, vol. 86, pp. 213–222, 2014.
- [20] M. L. Shi, *AC Impedance Spectroscopy Principles and Applications*, National Defense Industry Press, Beijing, China, 2001.
- [21] Y. H. Shao, *Electrochemical Methods Fundamentals and Applications*, Chemical Industry Press, Beijing, 2005.
- [22] C. N. Cao and J. Q. Zhang, *An Introduction to Electrochemical Impedance Spectroscopy*, Science Press, Beijing, China, 2002.



Hindawi
Submit your manuscripts at
www.hindawi.com

